

# Extraction of Distinguished Hyperbolic Trajectories for 2D Time-Dependent Vector Field Topology – Supplemental Material

Lutz Hofmann  and Filip Sadlo 

Heidelberg University, Germany

This document provides supplemental material for our paper “Extraction of Distinguished Hyperbolic Trajectories for 2D Time-Dependent Vector Field Topology”.

## 1. Continuous SVD Method

The singular value decomposition,

$$\mathbf{X}_{t_0}(t) = \mathbf{B}_{t_0}(t) e^{\mathbf{Z}_{t_0}(t)} \mathbf{R}_{t_0}(t)^\top, \quad (1)$$

of the fundamental solution matrix  $\mathbf{X}_{t_0}(t)$ ,

$$\frac{d}{dt} \mathbf{X}_{t_0}(t) = \mathbf{J}(t) \mathbf{X}_{t_0}(t), \quad \mathbf{X}_{t_0}(t_0) = \mathbb{I}, \quad (2)$$

is computed using the *continuous SVD method* by Dieci and Elia [DE08]. The main idea is to directly integrate in terms of the SVD, where the ODE can be formulated in the logarithms of the singular values, which capture the exponential separation. Equation 2 is integrated using a standard ODE solver for a short integration time only. At each time step  $t_i$ , we compute the singular value decomposition (Equation 1), and stop integration once  $\sigma_{t_0}^1(t_j) - \sigma_{t_0}^2(t_j) > 10^{-1}$  at a time step  $t_j$ . For integrating over the remaining time interval, the modified ODE [DE08] is given by

$$\frac{d}{dt} \mathbf{v}_1 = \mathbf{C}_{22}(t) - \mathbf{C}_{11}(t), \quad \mathbf{v}_1(t_j) = \sigma_{t_0}^2(t_j) - \sigma_{t_0}^1(t_j), \quad (3)$$

$$\frac{d}{dt} \mathbf{v}_2 = \mathbf{C}_{22}(t), \quad \mathbf{v}_2(t_j) = \sigma_{t_0}^2(t_j), \quad (4)$$

$$\frac{d}{dt} \mathbf{B} = \mathbf{B}(t) \mathbf{H}(t), \quad \mathbf{B}(t_j) = \mathbf{B}_{t_0}(t_j), \quad (5)$$

$$\frac{d}{dt} \mathbf{R} = \mathbf{R}(t) \mathbf{K}(t), \quad \mathbf{R}(t_j) = \mathbf{R}_{t_0}(t_j), \quad (6)$$

where the matrices  $\mathbf{C}(t)$ ,  $\mathbf{H}(t)$ ,  $\mathbf{K}(t)$  are defined as

$$\mathbf{C}(t) = \mathbf{B}(t)^\top \mathbf{J}(t) \mathbf{B}(t), \quad (7)$$

$$\mathbf{H}_{12}(t) = (\mathbf{C}_{12} \exp(\mathbf{v}_1(t)) + \mathbf{C}_{21}) / (\exp(\mathbf{v}_1(t))^2 - 1), \quad (8)$$

$$\mathbf{K}_{12}(t) = \exp(\mathbf{v}_1(t)) (\mathbf{C}_{12} + \mathbf{C}_{21}) / (\exp(\mathbf{v}_1(t))^2 - 1), \quad (9)$$

$$\mathbf{H}(t)^\top = -\mathbf{H}(t), \quad \mathbf{K}(t)^\top = -\mathbf{K}(t). \quad (10)$$

In order to keep the matrices  $\mathbf{B}(t)$  and  $\mathbf{R}(t)$  orthogonal, we replace them with the  $Q$ -factor of their  $QR$ -decomposition after each numerical integration step. We enforce a consistent orientation of

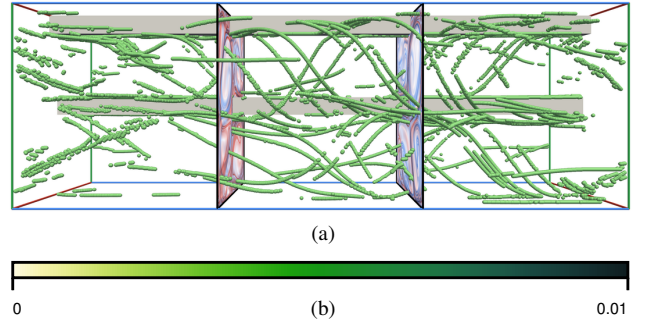


**Figure 1:** (a) Persistent local maxima (green) in the product of the forward and backward FTLE fields used as ground truth in the Convective Flow dataset. (b) Distance to ground truth in Figures 2d–2l.

the column vectors by multiplying  $Q$  with the diagonal matrix  $S = \text{diag}(\text{sign}(R_{11}), \text{sign}(R_{22}))$ , i.e., we rewrite  $QR = (QS)(SR)$ .

## 2. Convective Flow

In this section, we evaluate our method on the Convective Flow dataset. This is a CFD simulation of bouyant air flow with two obstacles. We extract the local maxima in the product of the forward and backward FTLE fields at a resolution of  $1000 \times 1000$  from 1001 equidistant points in time within the temporal domain [49s, 51s]. In order to obtain a reasonably noise-free ground truth for intersections of ridges in the forward and backward FTLE fields, we extract those local maxima, that have a persistence greater than 1000, which is approximately 10% (Figure 1a). As with the Cylinder Flow dataset (see Section 6.8 of the main paper), we found this method much more robust than extracting ridge lines or ridge surfaces at this FTLE resolution.

Much of the unsteady topology of the Convective Flow is generated by a slow moving DHT near the center of the domain. An initial candidate can be obtained by tracking critical points in the lab frame (Figure 2a). The Galilean invariant (Figure 2b), and the optimal reference frames (Figure 2c) are further able to extract candidates for the shorter, weaker DHTs, as well as some of the space-time separation and attachment lines at the no-slip boundaries. These additional candidates pose a challenge for both our

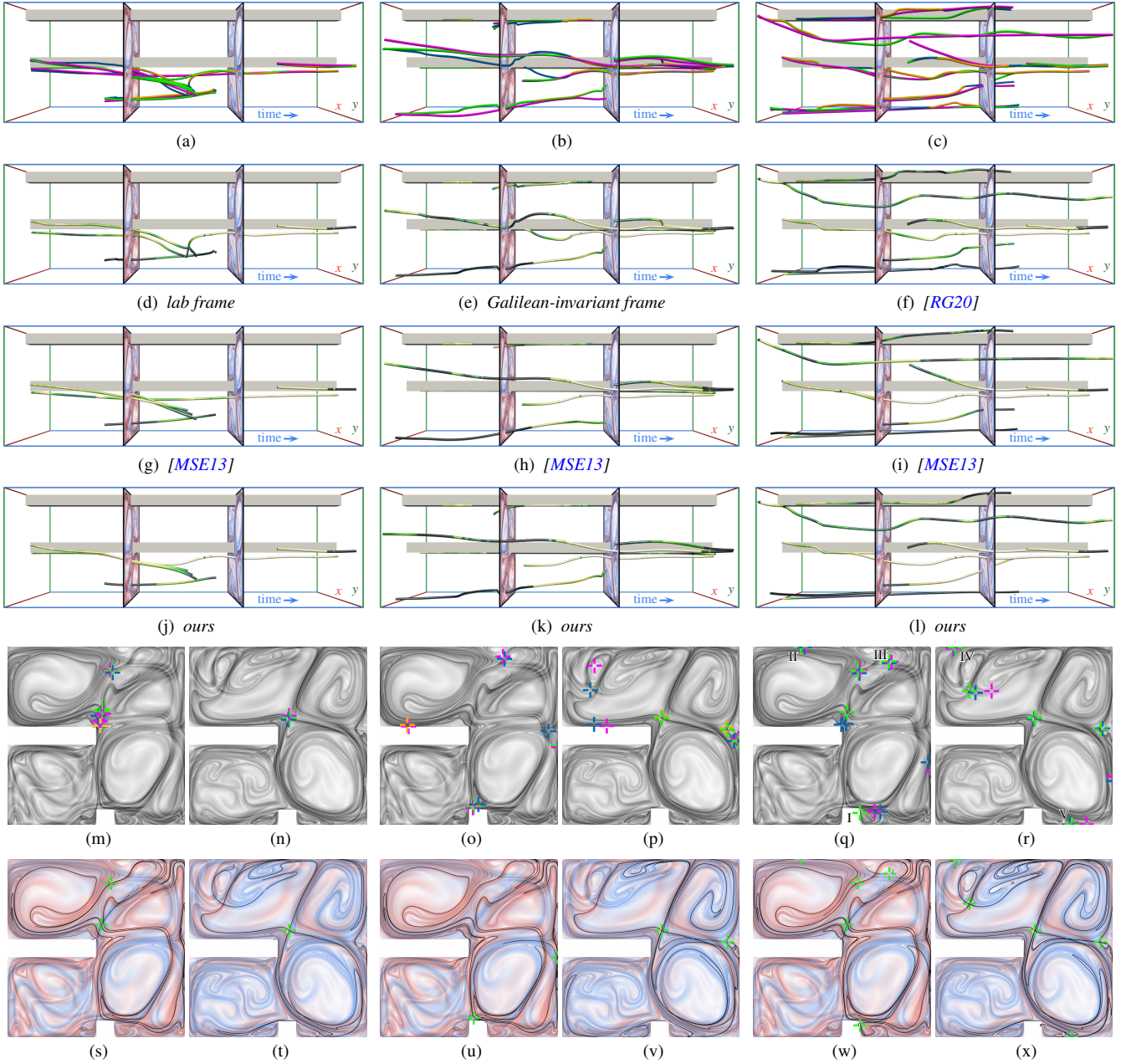


**Figure 2:** Extraction of DHTs in the Convective Flow. Initial line segments (orange), extended along the respective feature flow fields (blue), using critical points in the lab frame (a), with time slices (m)(n), in the Galilean-invariant frame of reference defined by the feature flow field (b), with time slices (o)(p), and in the optimal frame of reference [RG20] (c), with time slices (q)(r). The two time slices shown are at  $t=50$  s and  $t=51$  s, respectively. Initial candidates are corrected toward DHTs using local refinement [MSE13] (magenta) and our refinement (green). (d)–(l) Distance to nearest FTLE ridge intersection for each case (see Figure 1 for ground truth and color legend). (s)–(x) Streak manifolds computed from the obtained DHTs in each case (black lines) shown together with forward (red) and backward (blue) FTLE fields. (I, . . . , V) At candidate lines that are too close to the boundary or belong to weak DHT, the refinement does not reach FTLE ridge intersections.

DHT refinement and the bifurcation line refinement. While, in these cases, the latter seems to converge to arbitrary pathlines nearby, our DHT refinement reliably reaches either an attracting or repelling LCS, but not necessarily an intersection of both (I–V in Figures 2q and 2r). Near the boundary, both schemes can leave the spatial do-

main, since no spatial constraints are imposed by any of the methods. Therefore, we additionally extract separation and attachment lines as proposed by Machado et al. [MBES16] (shown in magenta in Figure 14 of the main paper). Initial candidates obtained from the optimal frame of reference [RG20] yield the most accurate results.

## References

- [DE08] DIECI L., ELIA C.: SVD algorithms to approximate spectra of dynamical systems. *Mathematics and Computers in Simulation* 79, 4 (2008), 1235–1254. [1](#)
- [MBES16] MACHADO G. M., BOBLEST S., ERTL T., SADLO F.: Space-time bifurcation lines for extraction of 2D Lagrangian coherent structures. *Computer Graphics Forum* 35, 3 (2016), 91–100. [2](#)
- [MSE13] MACHADO G. M., SADLO F., ERTL T.: Local extraction of bifurcation lines. In *Proc. Vision, Modeling and Visualization* (2013), pp. 17–24. [2](#)
- [RG20] ROJO I. B., GÜNTHER T.: Vector field topology of time-dependent flows in a steady reference frame. *IEEE Transactions on Visualization and Computer Graphics* 26, 1 (2020), 280–290. [2](#)